Research Article

PRNANO

ANDOVER HOUSE

Localized delivery of gel-embedded siRNA nanoparticles for pancreatic cancer treatment: Formulation, biodistribution, and bioactivity in mice

Majd Agbaria[a], Doaa Jbara-Agbaria[a], and Gershon Golomb[a,b]*

[a]Institute for Drug Research, School of Pharmacy, Faculty of Medicine, The Hebrew University of Jerusalem, Jerusalem 9112001, Israel
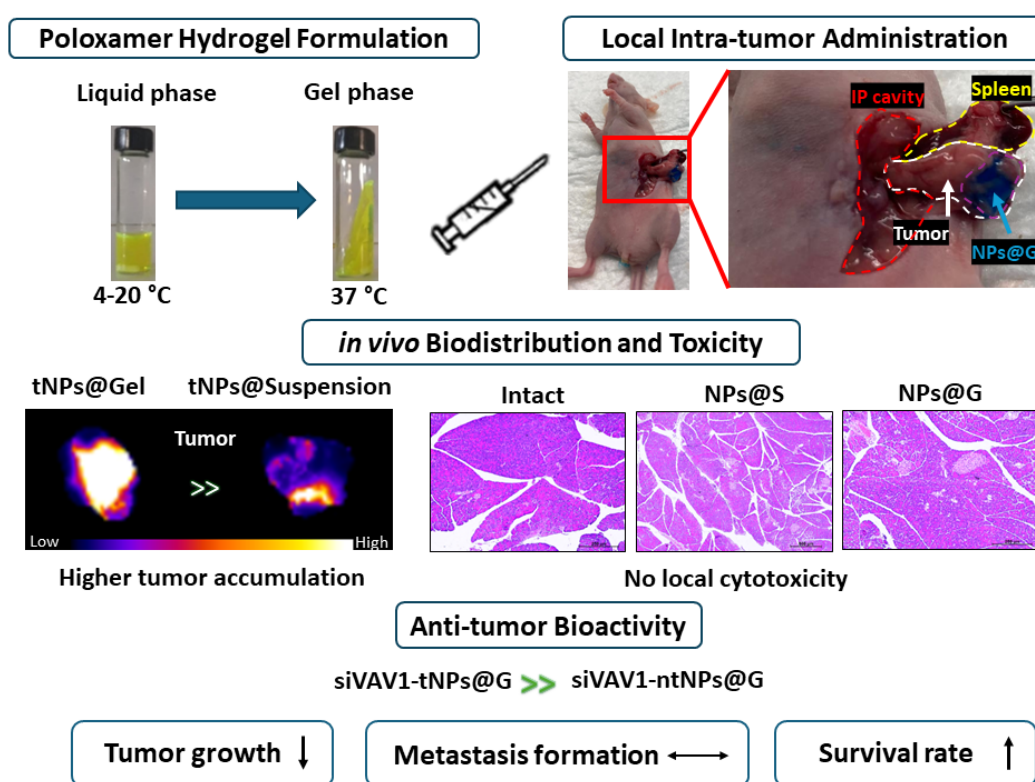*[b]The Center for Nanoscience and Nanotechnology, The Hebrew University of Jerusalem, Jerusalem 9190401, Israel*

Graphical Abstract

Abstract

Pancreatic cancer (PC) is one of the most lethal malignancies, primarily due to its dense extracellular matrix and poor vascularization, which limit effective drug accumulation and therapy. Here, we describe a local siRNA delivery system using thermosensitive hydrogel-embedded nanoparticles (NPs). siRNA against VAV1 (siVAV1), a key protein implicated in PC, was encapsulated in poly(lactic-co-glycolic acid) (PLGA)-based NPs decorated with an ApoB-derived peptide as the targeting ligand. The ApoB-targeted NPs exhibited optimal physicochemical properties, including nanoscale size, low poly-

---

* Corresponding Author: gershon.golomb@mail.huji.ac.il

dispersity index, and a neutral charge. The sustained-release siRNA-NPs were incorporated into a thermosensitive hydrogel (poloxamer) and locally injected into the pancreas of tumor-bearing mice. Treatment with targeted NPs in gel (tNPs@G) resulted in a notable increase in accumulation within the tumor (1.9-fold) and spleen (1.3-fold) 72 hours post-injection, with minimal systemic exposure and no local cytotoxicity. Intra-tumoral implantation of the gel-laden siVAV1 NPs in PC-bearing mice led to a significant reduction in tumor growth and volume (2.6-fold), mediated by the inhibition of both VAV1 mRNA and protein, and improved survival rates. The developed local siRNA delivery system provides a minimally invasive and effective therapeutic approach for PC, addressing key drug delivery barriers.

Rationale, Purpose, and Limitations

Pancreatic cancer (PC) remains one of the deadliest malignancies, primarily due to its dense stromal environment, poor vascularization, and resistance to conventional therapies. Gene therapy, particularly small interfering RNA (siRNA)-based approaches, holds great promise for PC treatment but faces significant barriers, including rapid degradation, poor tumor penetration, and off-target effects. To address these challenges, this study introduces a localized siRNA delivery system that integrates thermosensitive hydrogel-embedded nanoparticles (NPs) against VAV1, a protein implicated in PC progression. The NPs were decorated with an ApoB-derived peptide, enhancing tumor retention and accumulation. This approach aims to maximize local drug accumulation, minimize systemic exposure, and improve therapeutic efficacy in an orthotopic PC model. The localized siVAV1 delivery resulted in enhanced tumor targeting and efficacy. However, its efficacy against distant metastases was limited. The developed local siRNA delivery system provides a minimally invasive (e.g., by laparoscopy) and effective therapeutic approach for PC, addressing key barriers to drug delivery.

Introduction

PC is one of the most aggressive and fatal malignancies, with a 5-year survival rate of merely 10% [1-3]. This high mortality is driven by rapid disease progression, early metastatic spread, and late-stage diagnosis, which restricts surgical resection options to fewer than 20% of patients. The tumor's distinct microenvironment heightens this challenge, significantly hindering traditional treatments' effectiveness [4]. These limitations highlight an urgent need for alternative treatment strategies that can overcome the physical and physiological barriers of PC [4, 5].

siRNA-based therapeutic approach has emerged as a promising therapeutic modality for cancer, including PC [6-14]. siRNA enables precise gene silencing, disrupting key oncogenic pathways. The progress of RNA interference (RNAi)-based therapies is hindered by the very short half-life due to rapid degradation by blood nucleases, rapid clearance by the liver and kidneys, and inadequate cellular uptake because of their negative charge and large molecular weight. However, challenges such as inefficient NPs penetration into the dense tumor stroma, resulting in limited accumulation, and the potential for rapid clearance by the mononuclear phagocyte system (MPS) remain significant limitations. Therefore, to bypass the systemic delivery route hurdles, local implants of various drugs have been explored for enhanced therapy [15-19]. We hypothesized that a localized siRNA delivery system of targeted NPs embedded in a thermosensitive hydrogel could enhance drug retention and therapeutic efficacy in PC while minimizing systemic exposure and off-target effects.

VAV1, a hematopoietic signaling protein aberrantly expressed in tumor cells, has been identified as a novel and promising therapeutic target in PC due to its role in tumor progression and metastases [20-24]. Our earlier studies demonstrate that systemic administration of poly(lactic-co-glycolic acid) (PLGA)-based NPs containing siRNA against VAV1, siVAV1, effectively inhibits tumor growth and metastases in PC-bearing mice [23, 24]. Nevertheless, a local delivery system could enable sustained drug release at the tumor site, improving therapeutic efficacy while reducing systemic toxicity [15-19]. Thermosensitive and biodegradable hydrogels have been shown as promising local delivery systems [25-30]. Unlike polymeric implants, which require invasive procedures, injectable biodegradable hydrogels offer a minimally invasive approach through

laparoscopic techniques [31]. The thermosensitive gelling agent, poloxamer 407, has gained particular attention due to its ability to undergo sol-to-gel transition at physiological temperature, biocompatibility [32-37], and sensitizing multidrug-resistant cancer (MDR) cells [38, 39].

In this study, we developed a local siRNA delivery system of poloxamer gel-embedded NPs-laden siVAV1. To enhance the retention of the siVAV1 NPs in the pancreas, the NPs were decorated with an ApoB-derived peptide, a 25-amino-acid sequence from ApoB100 (SVKAQWKKNKHRHGCGRLTRKRGLK), specifically from amino acid residues 3145-3157 and 3359-3367. These segments were linked via a glycine-cysteine-glycine bridge [24, 40, 41]. The contribution of these peptide dimers to ApoB100's affinity for proteoglycans (PGs) and LDL receptors (LDLrs) is well established [42-48], which are abundantly expressed in PC cells and their extracellular matrix [49-51]. Here, we present this delivery system's formulation, characterization, and preclinical evaluation in an orthotopic PC mouse model.

Experimental Design

We hypothesized that enhanced therapeutic efficacy of PC could be achieved by local implantation of a thermosensitive hydrogel embedded with targeted NPs containing siRNA. We have developed targeted PLGA-based siRNA-loaded NPs against VAV1, a key protein implicated in PC progression, and embedded them into a thermosensitive poloxamer hydrogel to enable controlled and localized delivery. An orthotopic pancreatic tumor mouse model was selected for its clinical relevance, as it closely mimics the tumor microenvironment and disease progression seen in human PC. Animals were randomized into treatment groups receiving a gel loaded with targeted or non-targeted siRNA NPs via intra-tumoral injection. All experiments strictly followed ethical guidelines set by the Hebrew University of Jerusalem and the NIH (USA) (ethics approval number: MD-21-16763-5). The experimental strategy encompassed NPs formulation and characterization, hydrogel rheological assessment, in vivo biodistribution studies, evaluation of the therapeutic efficacy in terms of tumor growth suppression, survival rate, metastases for-

mation, and safety assessments, including histopathological analysis. This comprehensive, translational approach thoroughly evaluates gel-embedded siRNA NPs as a promising local delivery system for PC therapy.

Materials and Methods

All reagents were purchased from Sigma, Israel, unless stated otherwise.

PLGA-PEG-ApoB synthesis

The targeting peptide, ApoB (SVKAQWKKNKHRHGCGRLTRKRGLK, SynPeptide, China) [24, 40, 41], was linked to PLGA (PURASURB PDLG 5002, Corbion, The Netherlands) as previously described [24]. In short, following a redox reaction converting disulfide bonds to free thiol groups, ApoB was linked to PLGA-Polyethylene glycol-maleimide. The final product was confirmed by Fourier-transform infrared spectroscopy (FTIR, Nicolet 6700, Thermo Fisher Scientific, USA) and elemental analysis (Analytical chemistry lab, The Hebrew University of Jerusalem, Jerusalem, Israel). It was dialyzed, lyophilized, and kept at -20°C until further use.

Formulations of nanoparticles

Targeted (t) and non-targeted (nt) NPs were prepared as previously described [23, 24] by the double-emulsion solvent-diffusion (DESD) technique [52, 53]. The siRNA against VAV1 protein (21 base-pairs): sense: 5'-CGUCGAGGUCAAGCACAUUdTdT-3'; antisense: 5'-AAUGUGCUUGACCUCGAC-GdTdT-3' (1 mg/ml; Tamar Ltd., Israel) in RNase-free tris-EDTA (TE) buffer, was emulsified in ethylacetate:DMSO: acetonitrile, 65:20:15 containing 3% w/v PLGA and PLGA-PEG-ApoB (9:1 weight ratio), and the positively-charged counter ion, LL37 (GL Biochem, China) in an N:P ratio of 4 (nitrogen to siRNA's phosphate ratio). The solution was sonicated over an ice bath, and the resulting primary emulsion was added dropwise to TE buffer containing 2% w/v poloxamer 407, yielding double water in oil in water emulsion (W/O/W). The organic phase was evaporated, and the NPs were washed twice to remove excess poloxamer and free siRNA, re-suspended in a sterile 20% w/w poloxamer solution, lyophilized, and stored at -20°C until further use. NPs free of siRNA were prepared using the same procedure, omitting siRNA. Fluorescent

NPs were prepared by replacing 10% PLGA with PLGA-Cy5 (PolySciTech, Akina, Inc., IN, USA).

To prepare a suspension of NPs, the required amount of lyophilized nanoparticle powder was re-suspended in TE buffer under gentle agitation to ensure uniform particle dispersion.

For formulating NPs in a gel, a pre-weighed amount of poloxamer 407 was slowly added to the cold NPs suspension under stirring. The mixture was then stored at 4°C overnight to allow complete dissolution and uniform distribution of poloxamer 407, forming a stable 20% w/w thermosensitive gel-laden NPs.

Physicochemical characterization

Size and surface charge

An aliquot (20 μL) of the suspension or gel of nanoparticles was added to 1 mL of TE buffer. NPs size, polydispersity index (PDI), and surface charge (zeta potential) were determined by dynamic light scattering (DLS) at 4°C (Zetasizer Nano-ZSP, Malvern Instruments, UK).

siRNA release

Free siVAV1 or siVAV1 NPs in the gel were placed at the bottom of test tubes for 30 min at 37°C to form a stable gel. Pre-warmed TE buffer (1 mL; 37°C), containing 0.1% w/v Tween and 1 mg/mL heparin, pH 7.4, was gently added above the formed gels under shaking (30 rpm). The release medium was collected and replaced with an equal volume of fresh TE buffer in duplicates at each time point. To determine siVAV1 release from the NPs in suspension, duplicate test tubes for each time point containing 1 ml of the NP suspension were shaken at 37°C. At each time point, the NPs were separated from the medium by ultracentrifugation (45000 rpm). siVAV1 concentration in the supernatant was determined using ultraviolet spectrophotometry (NanoDrop) at 260 nm.

Rheological properties of the gel

The rheological behavior of the gel was assessed over a temperature range of 4–37°C using a parallel-plate geometry rheometer (Anton Paar MCR 101, Germany). The measurements were conducted with a 25 mm parallel plate geometry and a fixed gap of 0.5 mm, ensuring proper and uniform sample loading. A temperature-controlled system maintained and stabilized the sample at each desired temperature. The gel's flow properties were investigated by applying an increasing shear rate from 100 to 7000 s^{-1}, and the viscosity was continuously measured over the shear rate range to characterize the flow behavior.

Orthotopic PC mouse model

Animal Care

Animal care and procedures adhered to the standards for the care and use of laboratory animals established by the Hebrew University of Jerusalem, Israel, and the National Institutes of Health (NIH, USA; ethics approval number, MD-21-16763-5). Animals were provided with standard laboratory chow and tap water ad libitum.

Lentiviral overexpression of luciferase and GFP (green fluorescence protein)

All cell culture reagents were purchased from Biological Industries (Sartorius, Beit-Haemek, Israel). Dan-G cells, a human pancreatic adenocarcinoma cell line (DSMZ, Germany), were routinely cultivated in RPMI-1640 medium supplemented with 10% fetal bovine serum (FBS), 2 mM L-glutamine, 100 units/ml penicillin, and 100 μg/ml streptomycin (37°C, 5% CO_2).

Dan-G cells were transduced by a lentiviral vector (pLVX-Luc and pLVX-eGFP) for a stable expression of firefly luciferase (LUC) and GFP, as previously described [23, 24]. Briefly, HEK293T cells were seeded and transfected with the lentiviral vector and packaging plasmids by calcium precipitation. A mix of VSV-G (vesicular stomatitis virus glycoprotein; viral envelope), gag-pol (Δ8.9 for lentiviral vector), lentiviral vector (pLVX-EF1a-IRES-Puro; NovoPro, China), and 0.5 M CaCl2 was prepared in 2.5 mM HEPES pH 7.5. The mix was added dropwise on HEK293T cells, and after the medium change, the supernatant of the virus-producing HEK293T cells was collected. Dan-G cells were incubated overnight with the viral supernatant, followed by medium replacement and selection by puromycin. A similar transduction protocol was followed for GFP expression, and GFP$^+$ was sorted by flow cytometry (BD FACSAria III Sorter, BD Biosciences, Canada).

Mouse PC model

As previously described, [23, 24], an orthotopic mouse PC model was used to evaluate the bioactivity and biodistribution of NPs@G following intra-tumor administration. Since the tumorized pancreas is a single continuous tissue with no visible boundary, treatments were injected into the pancreas/tumor tissue. A detailed schematic representation of the experimental setup is shown in Figure S2. The localization of the pancreas and tumor was performed as described [54], with some modifications. A small incision was made on the left abdominal flank to locate the pancreas/tumor, and the underlying muscle was gently elevated and incised to access the abdominal cavity, avoiding injury of organs. The muscle incision was extended, revealing the spleen. The pancreas/tumor and spleen were carefully exteriorized, and the pancreas/tumor was retracted laterally (Figure S1a). A needle was inserted into the pancreas of female athymic nude mice (7-8 weeks old, Harlan Laboratories, Israel) to inoculate the Dan-G$^{Luc/GFP}$ PC cells (0.5×10^6 cells in 20 µl of Matrigel, Corning, AZ, USA) forming a fluid-filled bubble in the pancreatic parenchyma. After removing the needle, the pancreas was left outside for a few min to check for possible hemorrhage or leakage. The organs are then returned to the peritoneal cavity, and the muscle and skin layers are stitched separately.

NPs' bioactivity in pancreatic tumor-bearing mice

An orthotopic mouse PC model was adopted as previously described [23, 24]. Tumor growth was monitored weekly via bioluminescence for up to 60 days. D-luciferin (150 mg/kg, Carbosynth Ltd., UK) was injected intraperitoneally, and the luminescence was measured 10 min later using IVIS Spectrum imaging system (PerkinElmer, Inc., MA, USA) and analyzed with Living Image software (PerkinElmer, Inc., MA, USA). Two weeks post-inoculation, the bioluminescence signal reached approximately 10^7 p/s. Based on the data obtained at sacrifice time points, this represents a tumor size of 0.05 to 0.1 cm³ (a similar correlation was reported in the literature [55]). Mice were randomly assigned to four treatment groups: siVAV1-tNPs@G (n=6), empty NPs@G (n=5), siVAV1-ntNPs@G (n=6), and siVAV1-Lipofectamine@G (n=5) prepared according to the manufacturer's protocol (Thermo Fisher Scientific, USA). See Figures S1 and S2 for the detailed experimental outline. A single intra-tumor injection (150 µg/mouse of siVAV1) was administered on day 14, following the surgical procedure described above, exposing the tumor for injection. Mice were euthanized upon reaching the humane endpoints (10% weight loss over 2 days or 20% total weight loss or any other signs of distress). Survival rates were expressed using the Kaplan-Meier curve.

Quantification of mRNA levels in tumors

Tumor samples were embedded in TRI reagent solution and homogenized, and total RNA was isolated per the manufacturer's protocol, as we previously described [23, 24]. RNA concentration was determined using NanoDrop 1000 (Thermo Fisher Scientific). cDNA was synthesized from 1 mg of extracted RNA, and VAV1 and GAPDH mRNA levels were quantified by SYBR green-based quantitative real-time polymerase chain reaction (qRT-PCR), using the CFX Connect Real-Time PCR Detection System (Bio-Rad, CA, USA). Primers sequences used: human VAV1, forward: 5'-TGG CAA GGT CAT CTA CAC CCT-3'; reverse: 5'-TCG TCG ATC TGG TCG GAC A-3'; human GAPDH, forward: 5'-TCA AGC TCA TTT CCT GGT ATG-3', reverse: 5'-GTG GTC CAG GGG TCT TAC TC-3'. Thermal cycling included 95°C for 10 min, followed by 40 cycles at 95°C for 5 s and 60°C for 15 s. Results are expressed as relative gene expression normalized to GAPDH and siVAV1-lipofectamine@G treated animals.

Semi-quantitative analysis of protein levels in tumors (Western blot)

As previously described [23, 24], tumors were lysed in radio-immunoprecipitation lysis buffer (RIPA; supplemented with protease and phosphatase inhibitors), cleared by centrifugation, mixed with Laemmli buffer, and protein concentrations determined by QPRO-BCA Kit (Cyanagen Reagents for Molecular Biology, Italy). Equal protein amounts were separated on SDS-PAGE gel and transferred onto polyvinylidene difluoride membranes (Merck, Ireland) using PowerPac basic power supply (Bio-Rad, CA, USA). The membranes were blocked with 5% w/v skim milk in tris-buffered saline/tween 20 buffer (TBS-T buffer) and then with rabbit primary Abs, VAV1 (ab97574, Abcam, MA,

USA), and β-actin (#4967, cell signaling technology, MA, USA). After washing with TBS-T buffer, the membranes were incubated with HRP-conjugated secondary goat anti-rabbit (Jackson ImmunoResearch, Inc., ab111-035-144, PA, USA). Ag/Ab complexes were visualized using an ECL detection kit (Immobilon Crescendo Western HRP Substrate, Millipore, USA), and β-actin was used as the loading control. Blots were developed by Bio-Rad Chemi-Doc XR (Bio-Rad, CA, USA) and analyzed by Image Lab software (Bio-Rad, CA, USA), followed by quantification of the bands' intensity using the ImageJ software.

Metastatic grade

Mice were monitored and euthanized at the pre-determined endpoints. Metastases formation in distal organs, liver, lungs, and guts was evaluated by means of the Typhoon FLA 9500 (GE Healthcare, UK) for GFP fluorescence (λ_{Ex}=488 nm, λ_{Em}=510 nm), followed by quantification by image analysis (ImageJ software) that was normalized to siVAV1-lipofectamine@G treated animals.

Biodistribution studies in pancreatic tumor-bearing mice

NPs biodistribution was examined in a pancreatic tumor-bearing mice model (for the detailed experimental setup, see Figure S2b). Two weeks after PC inoculation, a single intra-tumor implantation of fluorescently labeled (PLGA-Cy5) empty tNPs@S (n=8), tNPs@G (n=8) and saline (n=4) were administered, following the surgical procedure described above exposing the tumor for injection (150 μg/mouse of siVAV1, equivalent to the total dose administered in the bioactivity study; Figure. S2a). Mice were euthanized 24- and 72-h following treatment, and blood and organs were analyzed for NPs accumulation using fluorescence imaging (Typhoon FLA 9500, GE Healthcare, UK) followed by image analysis (ImageJ software). The mean fluorescent intensity obtained was normalized to the auto-fluorescence in the saline-treated group.

In addition, we took advantage of the euthanized animals in the bioactivity experiment (see the experimental setup in Figure S2a), which reached the humane endpoints, and examined NPs biodistribution. The accumulation of the NPs in the harvested organs was examined on days 10-21 following the gel implantation. Organs were analyzed for NPs accumulation using fluorescence imaging (Typhoon FLA 9500, GE Healthcare, UK) and image analysis (ImageJ software). The mean fluorescent intensity was normalized to the auto-fluorescence in the siVAV1-Lipofectamine@G treated mice.

Uptake by monocytes

NPs uptake by monocytes was examined in a pancreatic tumor-bearing mice model (see the experimental setup in Figure S2b). Blood was collected, vortexed with HPLC-grade water, followed by the addition of 5% w/v bovine serum albumin (BSA) in ×10 PBS to remove erythrocytes, and centrifuged (400 g, 10 min) as previously described [23, 24]. Circulating monocytes ($CD11b^+$/$Ly-6C^+$) were incubated with V450-labeled anti-CD11b (1:200, BD Biosciences) and FITC-labeled anti-Ly-6C (1:200, BD Biosciences), or isotype controls. Cells were re-suspended in 0.5% w/v of BSA and analyzed by flow cytometry (CytoFlex S, Beckman Coulter, Inc., IN, USA) for Cy-5 positive cells. Saline-treated animals were used as controls. The number of stained cells and their fluorescent intensities were calculated from the histograms obtained (CytExpert software 2.3, Beckman Coulter, Inc., IN, USA).

Statistical Analysis

All data are expressed as the mean ± standard deviation unless noted otherwise. The one-way analysis of variance (ANOVA) with Tukey's post hoc analysis was used for statistical analysis. Differences were considered significant at $p < 0.05$.

Results

NPs in gel characterization

Targeted (t) and non-targeted (nt) PLGA-based NPs containing siVAV1 were successfully synthesized. They exhibit a mean diameter of approximately 100 nm, a narrow size distribution, and a neutral surface charge (Table 1). No significant changes in these key parameters were observed after incorporating both types of NPs into the gel (Table 1).

Gel rheology

The rheological properties of NPs-loaded gel (NPs@G) were evaluated across various temperatures. The gel remained liquid at 4-20°C but transitioned to a gel-like phase at tempera-

tures above 20°C (Figure 1a). The same rheological behavior was obtained following the incorporation of the NPs into the gel compared to the blank gel (Figure 1b-e). Within the 4–20°C range, gels exhibited constant viscosity despite increasing shear rates, indicating a Newtonian behavior (Figure 1b and d). Of note, at 20°C, an increase in viscosity of both gel types was observed (Figure 1b and d). Nevertheless, at higher temperatures (25- and 37°C), both gels exhibited decreased viscosity plastic rheological behavior as the shear rate increased (Figure 1c and e).

Table 1. The Physicochemical Properties of NPs in Gel

Formulation	Size (nm)	PDI	Zeta Potential (mv)
siVAV1-tNPs@suspension	123.2 ± 1.6	0.16 ± 0.03	0.4 ± 0.1
siVAV1-tNPs@gel	122.8 ± 0.8	0.16 ± 0.02	0.6 ± 0.4
siVAV1-ntNPs@suspension	98.5 ± 0.5	0.28 ± 0.07	−2.0 ± 0.8
siVAV1-ntNPs@gel	100.1 ± 5.3	0.33 ± 0.02	−1.9 ± 0.5

NPs=nanoparticles; PDI=polydispersity index; Mean ± SD
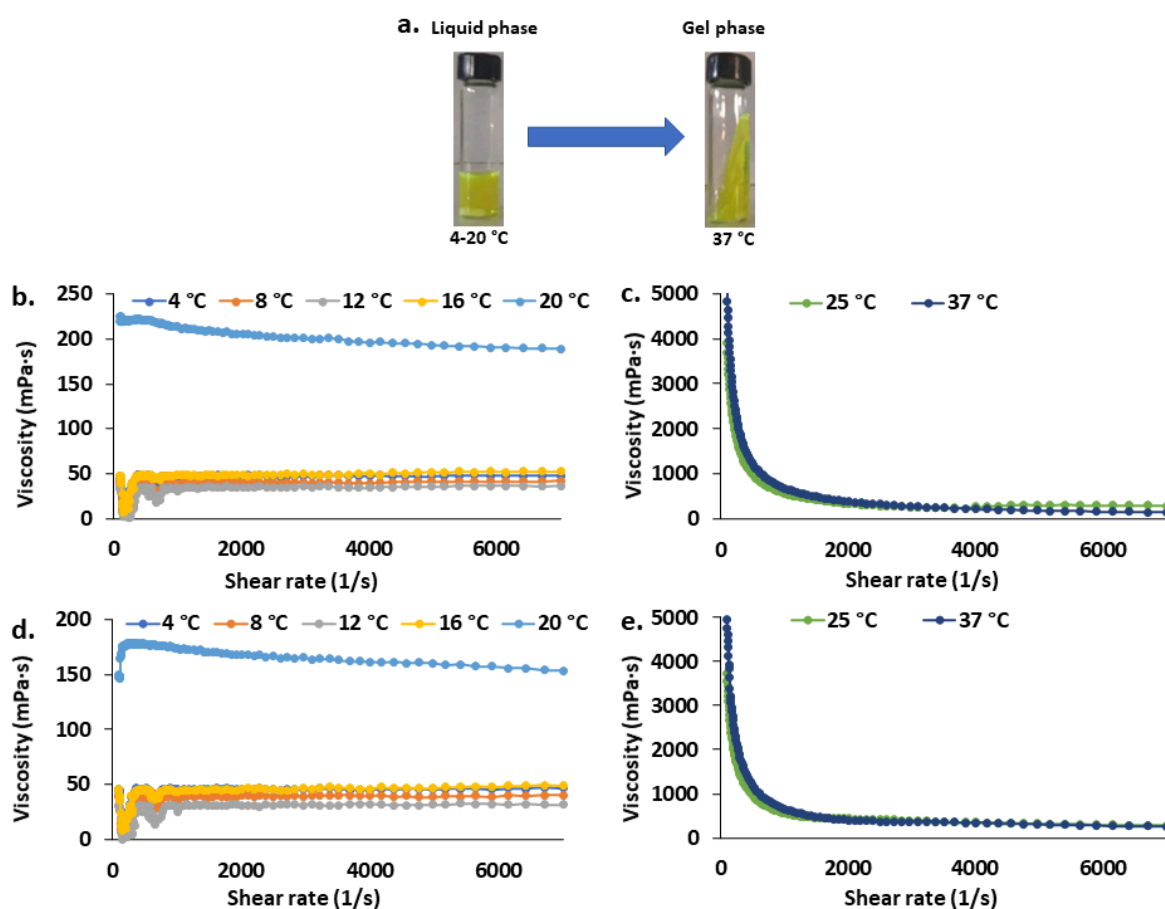
Figure 1. Rheological properties of the gel. a) A photomicrograph illustrating the phase transition from liquid (4–20°C) to gel (37°C). The viscosities of the blank gel (b-c) and NPs-loaded gel (d-e) were assessed across a broad temperature range (4–37°C).
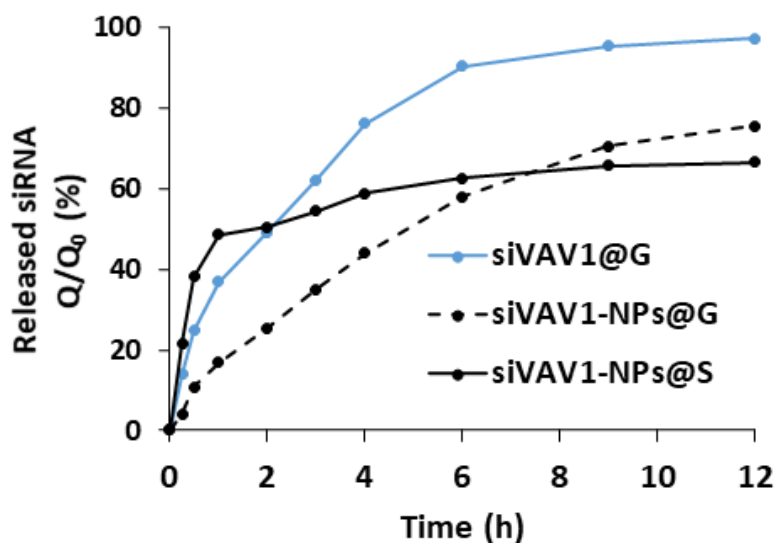

Figure. 2. The release profile of siVAV1 from NPs in gel (siVAV1-NPs@G) in comparison to free siVAV1 in gel (siVAV1@G) and to siVAV1 in NPs suspension (siVAV1-NPs@S). The NPs were separated from the medium by ultracentrifugation, and the amount of siRNA in the supernatant was quantified by means of UV spectrophotometry (Nanodrop). Mean ± SD

siRNA release

The suspension of siVAV1-loaded NPs (siVAV1-NPs@S) exhibited an initial burst effect; 40% of siVAV1 were released within the first 30 min, followed by a steady-state release with 66% after 12 h. In contrast, a gradual and exponential rate of 100% release after 12 h was observed from the free siVAV1 formulated in gel (siVAV1@G). siVAV1-loaded NPs in gel (siVAV1-NPs@G) exhibited a similar but slower release kinetics pattern of the siRNA, with 75% released after 12 hours (Figure 2).

NPs biodistribution following implantation

Local injection of tNPs@G in the tumor resulted in relatively high accumulation in the spleen and tumor after 24 and 72 h, similar to tNPs@S administration (Figure 3). Although no significant accumulation differences were observed across all examined organs between the formulations, a strong tendency of higher accumulation of the tNPs@G was noted in the spleen and tumor after 72 h, 1.3- and 1.9-fold, respectively (Figure 3).

NPs biodistribution was also evaluated in animals, reaching a humane endpoint in the bioactivity study. All types of NPs@G exhibited insignificant higher concentrations in the tumor for up to 21 days post-injection (Figure 4). Circulatory monocyte uptake (CD11b$^+$ and Ly-6C$^+$) by both formulations revealed similar low levels 24 h post-treatment, 21±8% and 17±2%, tNPs@S and tNPs@G, respectively (Figure 5b). A decreased uptake was noted after 72 h, declining to 1.5±1% and 7±6%, tNPs@S and tNPs@G, respectively (Figure 5b). Both formulation types displayed high plasma levels 24 h post-treatment, significantly decreasing after 72 h (Figure. 5c).
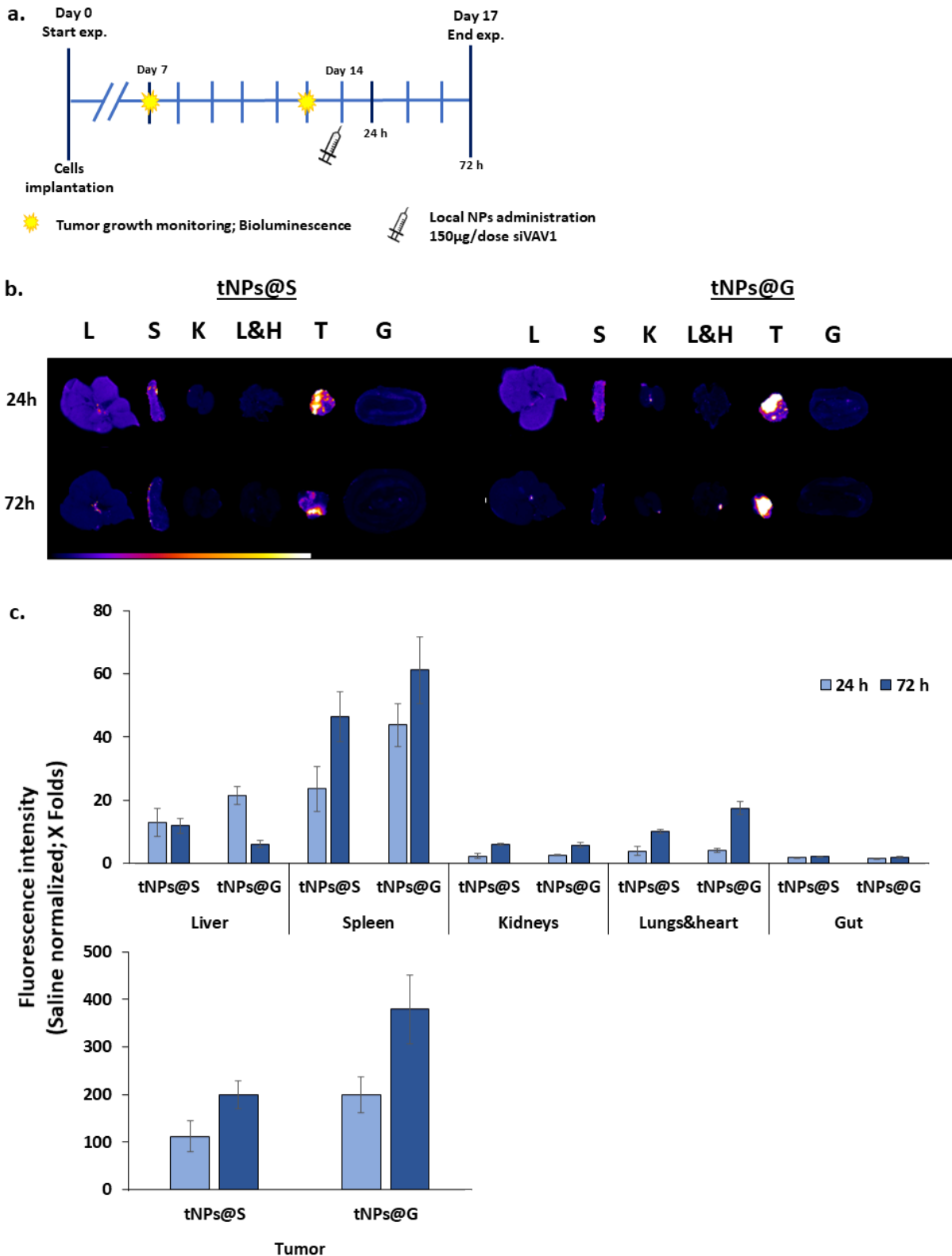
Figure 3. The biodistribution of targeted NPs in gel (tNPs@G) in comparison to targeted NPs in suspension (tNPs@S) following treatment (single intra-tumor injection) in pancreatic tumor-bearing mice. a) Experimental setup of the biodistribution study (see Figure S2b for more details). b) Representative biodistribution images, c) Fluorescence intensity analysis. The organs, L&H (lungs & heart), K (kidneys), S (spleen), L (liver), G (Gut), and T (tumor), were harvested after 24 and 72 h and analyzed using a Typhoon scanner. (n=4 at each timepoint; mean ± SEM).
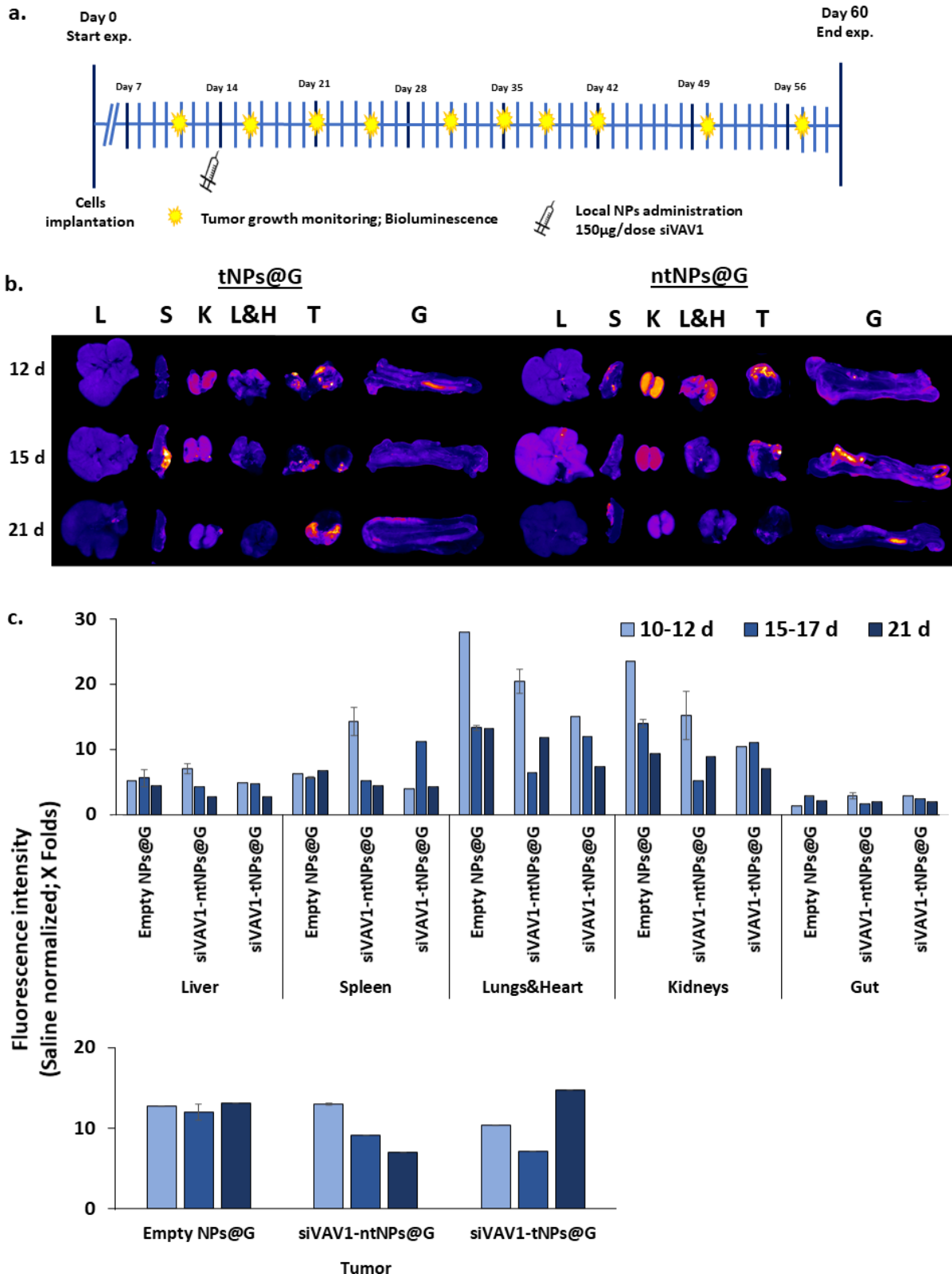
Figure 4. NPs biodistribution following gel-embedded targeted and non-targeted NPs (tNPs@G and ntNPs@G) treatments of mice in the bioactivity study reaching humane endpoints. a) Experimental setup of the bioactivity study (see Figure S2a for more details). b) Representative biodistribution images. c) Fluorescence intensity analysis. The organs, L&H (lungs & heart), K (kidneys), S (spleen), L (liver), G (Gut), and T (tumor) were harvested and examined using a Typhoon scanner. (n=1-3 at each timepoint; Mean ± SEM).
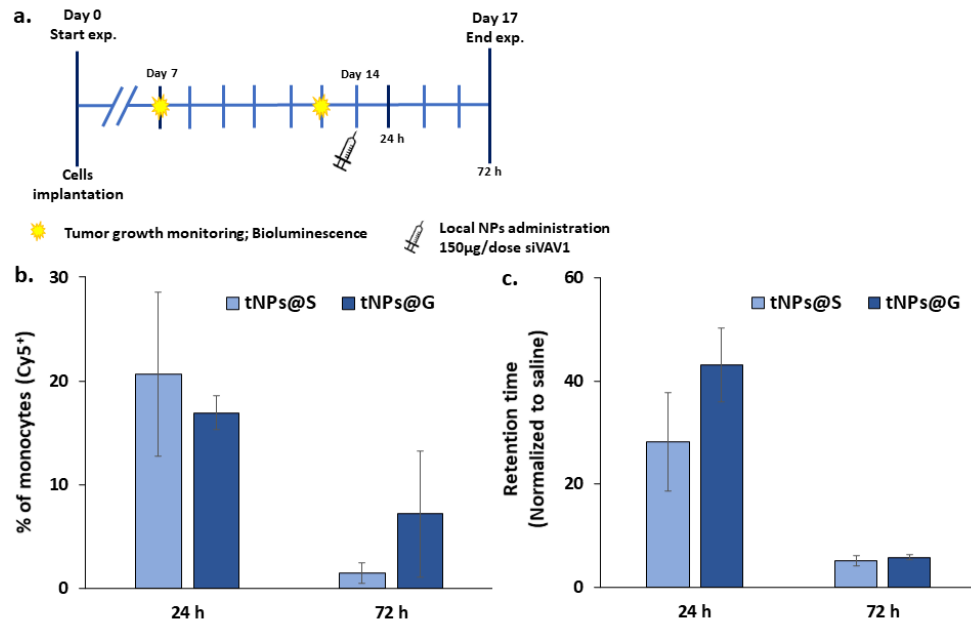
Figure 5. NPs circulatory retention time and uptake by monocytes following treatment (single intra-tumor injection) with targeted NPs in gel (tNPs@G), in comparison to targeted NPs in suspension (tNPs@S) in pancreatic tumor-bearing mice. a) Experimental setup for the biodistribution study (see Figure S2b for more details). Blood specimens were analyzed 24 and 72 h after treatment for monocyte uptake (b) and retention time in plasma (c) using flow cytometry and a Typhoon scanner, respectively. (n=4 at each time point; mean ± SEM).

Local cytotoxicity of implanted gels

The possible tissue cytotoxicity of the gel was assessed in intact mice. Histological analysis 48 h after implantation revealed no signs of toxicity on the pancreatic tissue across all treatments (Figure 6).

Bioactivity following local delivery

The bioactivity of local treatments on tumor growth was monitored up to 60 days after tumor inoculation (for the detailed experimental setup, see Figure S2a). Only the treatment with siVAV1-tNPs@G reduced tumor growth rate and size (2.6-fold) compared to all other treatment groups (Figure 7b-c). Moreover, siVAV1-tNPs@G treatment resulted in a higher survival rate, though statistically insignificant, compared to all other treatment groups. Half of the mice survived beyond three weeks post-implantation, compared to 100% mortality observed in all other treatment groups (p=0.09, Figure 7d). The successful therapeutic effect of siVAV1-tNPs@G significantly reduced the tumor's VAV1 mRNA and protein levels (80±9% and 49±9%, respectively; Figure 7e-f). In contrast, the empty NPs group exhibited relatively higher VAV1 mRNA levels (~2.5-fold) than the siVAV1-Lipofectamine@G group, and no tumor inhibition was obtained.
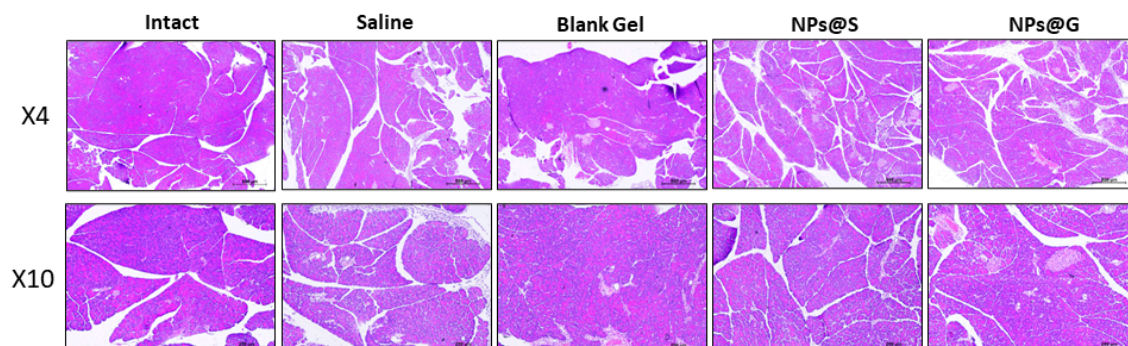

Figure 6. Local cytotoxicity of implanted gel-embedded NPs (NPs@G) in the pancreas of intact mice in comparison to blank gel, NPs suspension (NPs@S) and saline treatments. Representative micrographs (×4 and ×10 magnification) of hematoxylin/eosin-stained sections 48 h following local implantation (n=2 in each group).
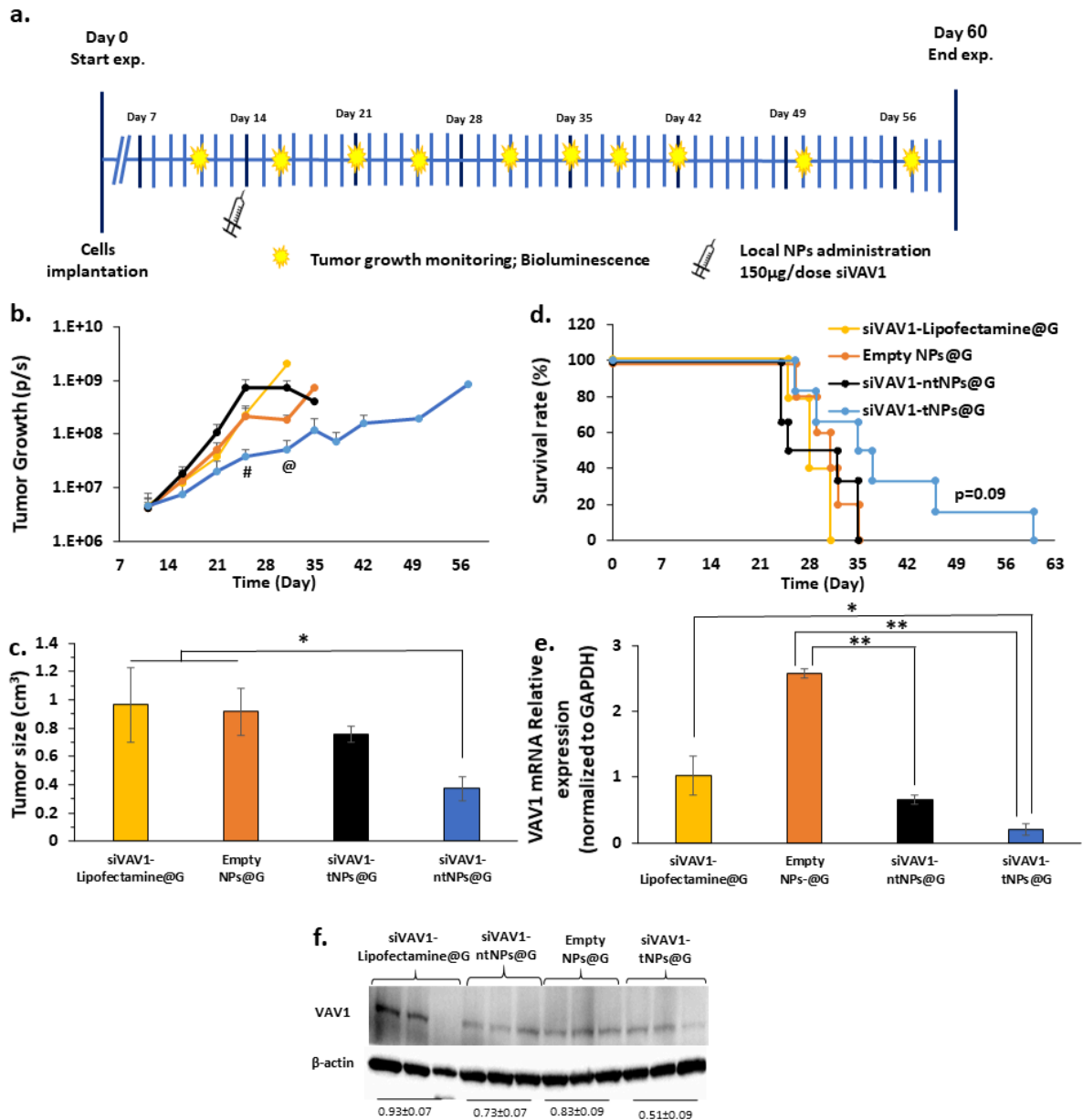
Figure 7. The bioactivity of non-targeted (nt) and targeted (t) NPs@G implants in comparison to siVAV1-lipofectamine@G following local injection in the pancreatic tumor-bearing mice model. a) Experimental setup of the bioactivity study (see Figure S2a for more details). b) Tumor growth rate, c) Tumor volume, and (d Kaplan-Meier survival curves. The knockdown of e) VAV1 mRNA and f) VAV1 protein levels in the tumors were evaluated using RT-PCR and western blot, respectively. VAV1 mRNA levels were normalized to GAPDH and siVAV1-Lipofectamine@G treated mice, and VAV1 protein levels were normalized to β-actin and siVAV1-Lipofectamine@G treated mice. n=5-6 in each treatment group; mean ± SEM. *p<0.05; **p<0.01; @p<0.01 vs. siVAV1-Lipofectamine@G; #p<0.05 vs. siVAV1-ntNPs@G.

The effect of NPs@G implants on metastases formation

Metastases formation in distal organs (liver, lungs, and gut) was evaluated by means of the GFP signal. None of the formulations affected metastatic grade in distal organs compared to the siVAV1-lipofectamine@G treatment group (Figure 8a-b).
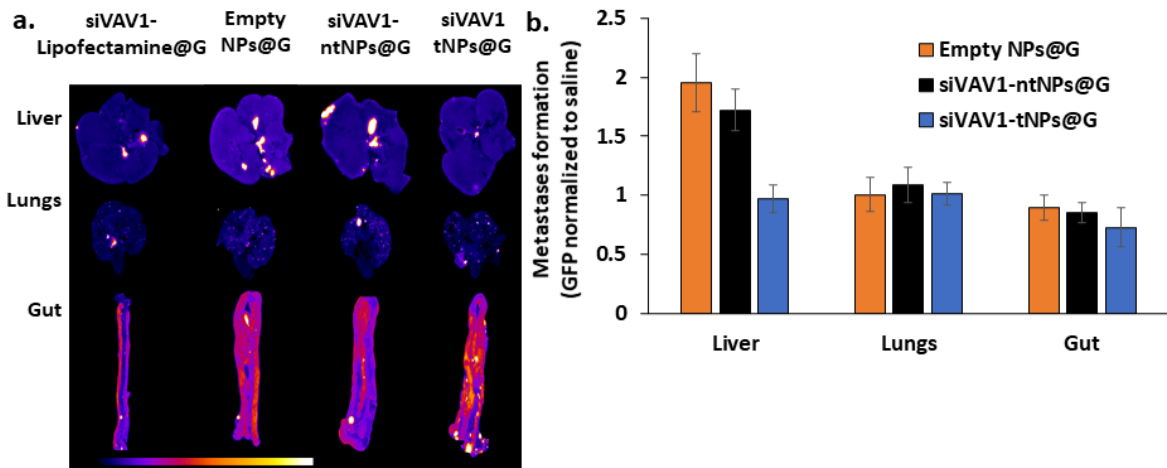
Figure 8. The effect of non-targeted (nt) and targeted (t) NPs@G implants in comparison to siVAV1-lipofectamine@G on metastases formation in the liver, lungs, and gut at sacrifice upon reaching humane endpoints (see Figure S2a for more detailed experimental setup). Representative images (a) and quantitative analysis (b) of metastases analyzed by means of GFP fluorescence, normalized to siVAV1-lipofectamine@G treated animals (n=5-6 in each treatment group; Mean ± SEM).

Discussion

Over the past few decades, identifying effective treatments for PC has remained a significant challenge, with very few drugs showing substantial efficacy [3]. Various strategies have been explored to overcome the challenges posed by chemotherapy-resistant PC, including nanomedicines [8-14, 56-58] and local implants [15-19]. In this study, we explored a treatment modality of a gel for the local delivery of siVAV1, which was encapsulated in ApoB-targeted NPs. We successfully developed a PLGA-based siRNA NPs formulation embedded in a thermosensitive gel system designed specifically for local PC therapy. This approach offers several key advantages, such as sustained siRNA release, enhanced tumor accumulation, and improved therapeutic outcomes in the challenging orthotopic PC model.

The targeted (t) and non-targeted (nt) NPs containing siVAV1 were successfully prepared using the DESD technique previously described by us for encapsulating siRNA [23, 24, 52, 53]. Spherical NPs approximately 100 nm in size, exhibiting a narrow size distribution and a neutral surface charge, have been successfully developed (Table 1). These neutral charge NPs possess optimal physicochemical properties, which are particularly advantageous for systemic and local administration [59-62]. Their neutral charge minimizes adverse interactions

with biological tissues, promoting enhanced localization and improving therapeutic efficacy in localized treatments.

We successfully incorporated these NPs into the poloxamer 407 hydrogel matrix without compromising their properties (Table 1). The rheological behavior of the poloxamer 407 hydrogel demonstrated a phase transition from liquid to hydrogel at physiological temperatures (Figure 1). Moreover, the gel maintained consistent viscosity at low temperatures while transitioning to a plastic-like behavior under physiological conditions (Figure 1). The siVAV1-NPs@G formulation exhibited a sustained-release profile, with 75% of siRNA released during 12 h, in contrast to the burst release observed in the suspension formulation, siVAV1-NPs@S (Figure 2). This controlled release, facilitated by the hydrogel matrix, ensures prolonged therapeutic exposure at the tumor site, thereby ensuring effective delivery and retention following local implantation. Poloxamers use is advantageous since they are effective in reversing and sensitizing MDR cancer cells by inhibiting the drug efflux transporter P-glycoprotein and modifying the micro-viscosity of the cellular membrane [39, 63]. Overall, the specific poloxamer used played a triple role as a surface-active agent, a cryoprotectant in preparing the siRNA-NPs, and as the gelling material. The favorable gelling properties and the release kinetics obtained attributes resulted in a

promising drug delivery system for local PC treatment, which can be used in a laparoscopy technique.

In this study, we employed the orthotopic mouse VAV1$^+$ PC model [23, 24], which appropriately reflects the tissue-specific pathology observed in primary tumors of human PC patients [64]. Biodistribution studies are essential for correlating accumulation with both safety and efficacy. It is reasonable to expect that a higher concentration of siRNA would be present in the tumor due to the longer retention time of NPs, which can be affected by the type of delivery vehicle and its targeting properties. Since the PLGA used begins to erode after approximately ~1-2 weeks, completely eroding after 4-6 weeks, the Cy5 signal primarily reflects intact NPs rather than degraded polymer. The primary biodistribution study's aim was to compare tumor retention of targeted NPs when delivered in suspension versus a gel delivery system (up to 3 days; Figure 3). Local intra-tumor administration of tNPs@G resulted, after 3 days, in a significant, though not statistically, increase in accumulation in the tumor (1.9-fold) and spleen (1.3-fold) compared to tNPs@S (Figure 3). An additional biodistribution study was conducted on animals that reached humane endpoints in the bioactivity study 10–21 days following treatment (Figure 4). The gel delivery system, whether for targeted or non-targeted NPs, demonstrated high tumor accumulation and prolonged retention, lasting up to three weeks after gel implantation (Figure 4). These findings indicate that employing gel-embedded NPs enhances local retention, facilitating sustained release of siVAV1. The enhanced tumor retention is likely attributed to the hydrogel's unique gelation properties, which promote localized retention at the implantation site. At the same time, the increased spleen accumulation may result from its anatomical proximity to the tumor and as a clearing organ for NPs [59-62]. Overall, the low plasma levels and minimal monocyte uptake observed 72 h post-implantation (Figure 5), combined with histopathological analysis of no signs of pancreatic tissue toxicity (Figure 6), indicate that the hydrogel formulation effectively limits systemic exposure and potential side effects.

Poloxamer 407 exhibits desirable thermosensitive properties that enable gelation near physiological temperatures, making it suitable for in

situ applications [33]. However, the application of poloxamer hydrogels in local cancer gene therapy has been reported only in breast cancer therapy [65, 66]. To our knowledge, this is the 1st report on a thermosensitive poloxamer hydrogel incorporating siRNA-loaded NPs for PC treatment.

In our previous study, an ApoB-targeted PLGA-based NPs encapsulating siVAV1 was developed, and effective therapy was achieved by 6 injections on alternate days (3 IP injections per week [24]). This study implemented a single intra-tumoral administration of a thermosensitive hydrogel following preliminary evaluations of dosing regimens. This method used only 50% of the total systemic dose (150 µg/mouse compared to 300 µg/mouse) to demonstrate the surpassing efficacy of the hydrogel formulation. As anticipated, the enhanced accumulation and retention of siVAV1-tNPs@G in the tumor resulted in significant tumor growth rate and volume suppression compared to the empty NPs@G and siVAV1-Lipofectamine@G (Figure 7b-c). Furthermore, this treatment improved survival, with 50% of mice surviving beyond three weeks post-implantation, in contrast to 100% mortality observed in all other treatment groups (p=0.09; Figure 7d). The successful therapeutic effect was associated with significantly reducing the tumor's VAV1 mRNA and protein levels (Figure 7e-f), consistent with our previous findings [23, 24]. As expected, the empty NPs group did not affect mRNA levels, resulting in higher VAV1 expression levels (~2.5) than the si-VAV1-Lipofectamine@G group. Moreover, both groups exhibited insignificant tumor inhibition, likely due to insufficient VAV1 knockdown. This aligns with the significantly lower VAV1 mRNA levels observed after siVAV1-tNPs@G treatment than the siVAV1-Lipofectamine@G and empty NP groups.

Unexpectedly, the siVAV1-ntNPs@G treatment showed neither effect on tumor growth or volume (Figure 7b-c) nor on mRNA and protein levels (Figure 5e-f). This apparent lack of anti-tumorigenic activity, in contrast to findings from our previous study [23], could be explained by the lower dosage employed in the current study and/or rapid elimination. Interestingly, this result underscores the rationale behind selecting a reduced dose to highlight the

superior efficacy of the targeted gel formulation. The enhanced effects of siVAV1-tNPs@G can be attributed to its increased accumulation and retention at the tumor site (Figure 3), mediated by the specific interaction between the targeting ligand (ApoB), PGs, and LDLrs, as previously reported by our group [24, 40, 41].

The rapid formation of metastases in PC is a major factor influencing survival outcomes, as they are a leading cause of mortality in this disease [1-3]. However, none of the treatments resulted in an anti-metastatic effect on distal organs (Figure 8), most probably due to the lack of accumulation in these organs. While the siVAV1@tNPs-G formulation demonstrated promising results in reducing tumor burden, its effect on metastatic grade was limited, most probably due to the timing of treatment and/or dose, which should be investigated in future research.

Conclusions

This study underscores the potential of targeted, gel-embedded siRNA NPs delivery systems in overcoming systemic and microenvironmental barriers associated with PC therapy, addressed by integrating sustained release, active targeting, and localized delivery. For local PC treatment, the PLGA-based siVAV1 NPs formulation embedded in a poloxamer thermosensitive hydrogel was successfully formulated. This approach demonstrated improved tumor targeting, accumulation, and retention. The hydrogel enables sustained siRNA release, effectively reducing tumor growth and improving survival rate, mediated via the reduction of both VAV1 mRNA and protein levels in the tumor in the orthotopic PC model. The lack of anti-tumor impact on metastases calls for further research.

Conflicts of Interest: The authors declare no conflict of interest. The funders had no role in the study's design, data collection, analysis, interpretation, manuscript writing, or decision to publish the results.

Quote this article as Agbaria, Majd, Doaa Jbara-Agbaria, and Gershon Golomb, "Localized Delivery of Gel-Embedded siRNA Nanoparticles for Pancreatic Cancer Treatment: Formulation, Biodistribution and Bioactivity in Mice." *Precision Nanomedicine*, 2005, 8(2), 1482–1500, https://doi.org/10.33218/001c.136412.

References

1. Ayres Pereira M, Chio IIC. Metastasis in pancreatic ductal adenocarcinoma: Current standing and methodologies. Genes-Basel. 2019;11(1). https://doi.org/10.3390/genes11010006.

2. Nakaoka K, Ohno E, Kawabe N, Kuzuya T, Funasaka K, Nakagawa Y, Nagasaka M, Ishikawa T, Watanabe A, Tochio T, Miyahara R, Shibata T, Kawashima H, Hashimoto S, Hirooka Y. Current status of the diagnosis of early-stage pancreatic ductal adenocarcinoma. Diagnostics. 2023;13(2). https://doi.org/10.3390/diagnostics13020215.

3. Jiang Y, Sohal DPS. Pancreatic adenocarcinoma management. JCO Oncol Pract. 2023;19(1):19-32. https://doi.org/10.1200/OP.22.00328.

4. Halbrook CJ, Lyssiotis CA, Pasca di Magliano M, Maitra A. Pancreatic cancer: Advances and challenges. Cell. 2023;186(8):1729-1754. https://doi.org/10.1016/j.cell.2023.02.014.

5. Kolbeinsson HM, Chandana S, Wright GP, Chung M. Pancreatic cancer: A review of current treatment and novel therapies. J Invest Surg. 2023;36(1):2129884. https://doi.org/10.1080/08941939.2022.2129884.

6. Hu B, Zhong L, Weng Y, Peng L, Huang Y, Zhao Y, Liang XJ. Therapeutic siRNA: State of the art. Signal Transduct Target Ther. 2020;5(1):101. https://doi.org/10.1038/s41392-020-0207-x.

7. Yu AM, Choi YH, Tu MJ. RNA drugs and RNA targets for small molecules: Principles, progress, and challenges. Pharmacol Rev. 2020;72(4):862-898. https://doi.org/10.1124/pr.120.019554.

8. Kim MJ, Chang H, Nam G, Ko Y, Kim SH, Roberts TM, Ryu JH. RNAi-based approaches for pancreatic cancer therapy. Pharmaceutics. 2021;13(10). https://doi.org/10.3390/pharmaceutics13101638.

9. Roacho-Perez JA, Garza-Trevino EN, Delgado-Gonzalez P, Z GB, Delgado-Gallegos JL, Chapa-Gonzalez C, Sanchez-Dominguez M, Sanchez-Dominguez CN, Islas JF. Target nanoparticles against pancreatic cancer: Fewer side effects in therapy. Life-Basel. 2021;11(11). https://doi.org/10.3390/life11111187.

10. Viegas C, Patricio AB, Prata J, Fonseca L, Macedo AS, Duarte SOD, Fonte P. Advances in pancreatic cancer treatment by nano-based drug delivery systems. Pharmaceutics. 2023;15(9). https://doi.org/10.3390/pharmaceutics15092363.

11. Luo W, Zhang T. The new era of pancreatic cancer treatment: Application of nanotechnology breaking through bottlenecks. Cancer Lett. 2024;594:216979. https://doi.org/10.1016/j.canlet.2024.216979.

12. Lara P, Quinonero F, Ortiz R, Prados J, Melguizo C. Nanoparticles bounded to interfering RNAs as a therapy for pancreatic cancer: A systematic review. Wiley Interdiscip Rev Nanomed Nanobiotechnol. 2024;16(6):e2013. https://doi.org/10.1002/wnan.2013.

13. Gu X, Minko T. Targeted nanoparticle-based diagnostic and treatment options for pancreatic cancer. Cancers. 2024;16(8). https://doi.org/10.3390/cancers16081589.

14. Moazzam M, Zhang M, Hussain A, Yu X, Huang J, Huang Y. The landscape of nanoparticle-based siRNA delivery and therapeutic development. Mol Ther. 2024;32(2):284-312. https://doi.org/10.1016/j.ymthe.2024.01.005.

15. Zorde Khvalevsky E, Gabai R, Rachmut IH, Horwitz E, Brunschwig Z, Orbach A, Shemi A, Golan T, Domb AJ, Yavin E, Giladi H, Rivkin L, Simerzin A, Eliakim R, Khalaileh A, Hubert A, Lahav M, Kopelman Y, Goldin E, Dancour A, Hants Y, Arbel-Alon S, Abramovitch R, Shemi A, Galun E. Mutant KRAS is a druggable target for pancreatic cancer. Proc Natl Acad Sci U S A. 2013;110(51):20723-20728. https://doi.org/10.1073/pnas.1314307110.

16. Golan T, Khvalevsky EZ, Hubert A, Gabai RM, Hen N, Segal A, Domb A, Harari G, David EB, Raskin S, Goldes Y, Goldin E, Eliakim R, Lahav M, Kopleman Y, Dancour A, Shemi A, Galun E. RNAi therapy targeting KRAS in combination with chemotherapy for locally advanced pancreatic cancer patients. Oncotarget. 2015;6(27):24560-24570. https://doi.org/10.18632/oncotarget.4183.

17. Indolfi L, Ligorio M, Ting DT, Xega K, Tzafriri AR, Bersani F, Aceto N, Thapar V, Fuchs BC, Deshpande V, Baker AB, Ferrone CR, Haber DA, Langer R, Clark JW, Edelman ER. A tunable delivery platform to provide local chemotherapy for pancreatic ductal adenocarcinoma. Biomaterials. 2016;93:71-82. https://doi.org/10.1016/j.biomaterials.2016.03.044.

18. Liu J, Wu W, Zhu Q, Zhu H. Hydrogel-based therapeutics for pancreatic ductal adenocarcinoma treatment. Pharmaceutics. 2023;15(10). https://doi.org/10.3390/pharmaceutics15102421.

19. Shi K, Xue B, Jia Y, Yuan L, Han R, Yang F, Peng J, Qian Z. Sustained co-delivery of gemcitabine and cis-platinum via biodegradable thermo-sensitive hydrogel for synergistic combination therapy of pancreatic cancer. Nano Res. 2019;12(6):1389-1399. https://doi.org/10.1007/s12274-019-2342-7.

20. Katzav S. Vav1: A Dr. Jekyll and Mr. Hyde protein--good for the hematopoietic system, bad for cancer. Oncotarget. 2015;6(30):28731-28742. https://doi.org/10.18632/oncotarget.5086.

21. Razidlo GL, Magnine C, Sletten AC, Hurley RM, Almada LL, Fernandez-Zapico ME, Ji B, McNiven MA. Targeting pancreatic cancer metastasis by inhibition of vav1, a driver of tumor cell invasion. Cancer Res. 2015;75(14):2907-2915. https://doi.org/10.1158/0008-5472.CAN-14-3103.

22. Salaymeh Y, Farago M, Sebban S, Shalom B, Pikarsky E, Katzav S. Vav1 and mutant K-Ras synergize in the early development of pancreatic ductal adenocarcinoma in mice. Life Sci Alliance. 2020;3(5). https://doi.org/10.26508/lsa.202000661.

23. Agbaria M, Jbara-Agbaria D, Grad E, Ben-David-Naim M, Aizik G, Golomb G. Nanoparticles of VAV1 siRNA combined with LL37 peptide for the treatment of pancreatic cancer. J Control Release. 2023;355:312-326. https://doi.org/10.1016/j.jconrel.2023.01.084.

24. Agbaria M, Jbara-Agbaria D, Golomb G. Targeting siRNA nanoparticles with ApoB Peptide: Formulation, biodistribution, and bioactivity in pancreatic tumor-bearing mice. J Drug Deliv Sci Technol. Volume 108, 2025:106900. https://doi.org/10.1016/j.jddst.2025.106900.

25. Gong C, Qi T, Wei X, Qu Y, Wu Q, Luo F, Qian Z. Thermosensitive polymeric hydrogels as drug delivery systems. Curr Med Chem. 2013;20(1):79-94. https://doi.org/10.2174/09298673311302010009.

26. Li Z, Guan J. Thermosensitive hydrogels for drug delivery. Expert Opin Drug Deliv. 2011;8(8):991-1007. https://doi.org/10.1517/17425247.2011.581656.

27. Norouzi M, Nazari B, Miller DW. Injectable hydrogel-based drug delivery systems for local cancer therapy. Drug Discov Today. 2016;21(11):1835-1849. https://doi.org/10.1016/j.drudis.2016.07.006.

28. Jeong B, Kim SW, Bae YH. Thermosensitive sol–gel reversible hydrogels. Adv Drug Deliver Rev. 2012;64:154-162. https://doi.org/10.1016/j.addr.2012.09.012.

29. Moon HJ, Ko du Y, Park MH, Joo MK, Jeong B. Temperature-responsive compounds as in situ gelling biomedical materials. Chem Soc Rev. 2012;41(14):4860-4883. https://doi.org/10.1039/c2cs35078e.

30. Marques AC, Costa PJ, Velho S, Amaral MH. Stimuli-responsive hydrogels for intratumoral drug delivery. Drug Discov Today. 2021;26(10):2397-2405. https://doi.org/10.1016/j.drudis.2021.04.012.

31. Shrikhande SV, Barreto SG, Shukla PJ. Laparoscopy in pancreatic tumors. J Minim Access Surg. 2007;3(2):47-51. https://doi.org/10.4103/0972-9941.33272.

32. Akash MS, Rehman K. Recent progress in biomedical applications of pluronic (PF127): Pharmaceutical perspectives. J Control Release. 2015;209:120-138. https://doi.org/10.1016/j.jconrel.2015.04.032.

33. Bodratti AM, Alexandridis P. Formulation of poloxamers for drug delivery. J Funct Biomater. 2018;9(1). https://doi.org/10.3390/jfb9010011.

34. Yu M, Zhang C, Tang Z, Tang X, Xu H. Intratumoral injection of gels containing losartan microspheres and (PLG-g-mPEG)-cisplatin nanoparticles improves drug penetration, retention and anti-tumor activity. Cancer Lett. 2019;442:396-408. https://doi.org/10.1016/j.canlet.2018.11.011.

35. Chung CK, Garcia-Couce J, Campos Y, Kralisch D, Bierau K, Chan A, Ossendorp F, Cruz LJ. Doxorubicin loaded poloxamer thermosensitive hydrogels: Chemical, pharmacological and biological evaluation. Molecules. 2020;25(9). https://doi.org/10.3390/molecules25092219.

36. Norouzi M, Firouzi J, Sodeifi N, Ebrahimi M, Miller DW. Salinomycin-loaded injectable thermosensitive hydrogels for glioblastoma therapy. Int J Pharmaceut. 2021;598:120316. https://doi.org/10.1016/j.ijpharm.2021.120316.

37. Marques AC, Costa PC, Velho S, Amaral MH. Injectable poloxamer hydrogels for local cancer therapy. Gels. 2023;9(7):593. https://doi.org/10.3390/gels9070593.

38. Batrakova EV, Kabanov AV. Pluronic block copolymers: Evolution of drug delivery concept from inert nanocarriers to biological response modifiers. J Control Release. 2008;130(2):98-106. https://doi.org/10.1016/j.jconrel.2008.04.013.

39. Kunjachan S, Rychlik B, Storm G, Kiessling F, Lammers T. Multidrug resistance: Physiological principles and nanomedical solutions. Adv Drug Deliv Rev. 2013;65(13-14):1852-1865. https://doi.org/10.1016/j.addr.2013.09.018.

40. Ben-David-Naim M, Dagan A, Grad E, Aizik G, Nordling-David MM, Morss Clyne A, Granot Z, Golomb G. Targeted siRNA nanoparticles for mammary carcinoma therapy. Cancers. 2019;11(4). https://doi.org/10.3390/cancers11040442.

41. Golomb G, Sacks H, Najareh Y, Fishbein E, Chorny M. Nanoparticles containing polymeric nucleic acid homologs. U.S. Patent US8178128B2. 2012.

42. Innerarity TL, Weisgraber KH, Rall SC, Mahley RW. Functional domains of apolipoprotein-E and apolipoprotein-B. Acta Med Scand. 1987:51-59. https://doi.org/10.1111/j.0954-6820.1987.tb09903.x.

43. Olsson U, Camejo G, Olofsson SO, Bondjers G. Molecular-parameters that control the association of low-density-lipoprotein apo-B-100 with chondroitin sulfate. Biochim Biophys Acta. 1991;1097(1):37-44. https://doi.org/10.1016/0925-4439(91)90021-Z.

44. Olsson U, Camejo G, HurtCamejo E, Elfsber K, Wiklund O, Bondjers G. Possible functional interactions of apolipoprotein B-100 segments that associate with cell proteoglycans and the apoB/E receptor. Arterioscl Throm Vas. 1997;17(1):149-155. https://doi.org/10.1161/01.Atv.17.1.149.

45. Borén J, Lee I, Zhu WM, Arnold K, Taylor S, Innerarity TL. Identification of the low density lipoprotein receptor-binding site in apolipoprotein B100 and the modulation of its binding activity by the carboxyl terminus in familial defective apo-B100. J Clin Invest. 1998;101(5):1084-1093. https://doi.org/10.1172/Jci1847.

46. Knott TJ, Pease RJ, Powell LM, Wallis SC, Rall SC, Innerarity TL, Blackhart B, Taylor WH, Marcel Y, Milne R, Johnson D, Fuller M, Lusis AJ, Mccarthy BJ, Mahley RW, Levywilson B, Scott J. Complete protein-sequence and identification of structural domains of human apolipoprotein-B. Nature. 1986;323(6090):734-738. https://doi.org/10.1038/323734a0.

47. Weisgraber KH, Rall SC. Human apolipoprotein B-100 heparin-binding sites. J Biol Chem. 1987;262(23):11097-11103.

48. Camejo G, Hurt-Camejo E, Wiklund O, Bondjers G. Association of apo B lipoproteins with arterial proteoglycans: Pathological significance and molecular basis. Atherosclerosis. 1998;139(2):205-222. https://doi.org/10.1016/S0021-9150(98)00107-5.

49. Kleeff J, Ishiwata T, Kumbasar A, Friess H, Buchler MW, Lander AD, Korc M. The cell-surface heparan sulfate proteoglycan glypican-1 regulates growth factor action in pancreatic carcinoma cells and is overexpressed in human pancreatic cancer. J Clin Invest. 1998;102(9):1662-1673. https://doi.org/10.1172/Jci4105.

50. Vasseur S, Guillaumond F. LDL receptor: An open route to feed pancreatic tumor cells. Mol Cell Oncol. 2016;3(1):e1033586. https://doi.org/10.1080/23723556.2015.1033586.

51. Furini S, Falciani C. Expression and role of heparan sulfated proteoglycans in pancreatic cancer. Front Oncol. 2021;11. https://doi.org/10.3389/fonc.2021.695858.

52. Ben David-Naim M, Grad E, Aizik G, Nordling-David MM, Moshel O, Granot Z, Golomb G. Polymeric nanoparticles of siRNA prepared by a double-emulsion solvent-diffusion technique: Physicochemical properties, toxicity, biodistribution and efficacy in a mammary carcinoma mice model. Biomaterials. 2017;145:154-167. https://doi.org/10.1016/j.biomaterials.2017.08.036.

53. Cohen-Sela E, Chorny M, Koroukhov N, Danenberg HD, Golomb G. A new double emulsion solvent diffusion technique for encapsulating hydrophilic molecules in PLGA nanoparticles. J Control Release. 2009;133(2):90-95. https://doi.org/10.1016/j.jconrel.2008.09.073.

54. Qiu W, Su GH. Development of orthotopic pancreatic tumor mouse models. Methods Mol Biol. 2013;980:215-223. https://doi.org/10.1007/978-1-62703-287-2_11.

55. Tuli R, Surmak A, Reyes J, Hacker-Prietz A, Armour M, Leubner A, Blackford A, Tryggestad E, Jaffee EM, Wong J, DeWeese TL, Herman JM. Development of a novel preclinical pancreatic cancer research model: Bioluminescence image- guided focal irradiation and tumor monitoring of orthotopic xenografts. Transl Oncol. 2012;5(2):77-84. https://doi.org/10.1593/tlo.11316.

56. Zhao X, Li F, Li Y, Wang H, Ren H, Chen J, Nie G, Hao J. Co-delivery of hif1α siRNA and gemcitabine via biocompatible lipid-polymer hybrid nanoparticles for effective treatment of pancreatic cancer. Biomaterials. 2015;46:13-25. https://doi.org/10.1016/j.biomaterials.2014.12.028.

57. Liu X, Lin P, Perrett I, Lin J, Liao Y-P, Chang CH, Jiang J, Wu N, Donahue T, Wainberg Z, Nel AE, Meng H. Tumor-penetrating peptide enhances transcytosis of silicasome-based chemotherapy for pancreatic cancer. J Clin Inves. 2017;127(5):2007-2018. https://doi.org/10.1172/JCI92284.

58. Bhatia SN, Chen X, Dobrovolskaia MA, Lammers T. Cancer nanomedicine. Nat Rev Cancer. 2022;22(10):550-556. https://doi.org/10.1038/s41568-022-00496-9.

59. Elazar V, Adwan H, Rohekar K, Zepp M, Lifshitz-Shovali R, Berger MR, Golomb G. Biodistribution of antisense nanoparticles in mammary carcinoma rat model. Drug Deliv. 2010;17(6):408-418. https://doi.org/10.3109/10717541003777225.

60. Moghimi SM, Hunter AC, Andresen TL. Factors controlling nanoparticle pharmacokinetics: An integrated analysis and perspective. Annu Rev Pharmacol. 2012;52:481-503. https://doi.org/10.1146/annurev-pharmtox-010611-134623.

61. Haroon HB, Hunter AC, Farhangrazi ZS, Moghimi SM. A brief history of long circulating nanoparticles. Adv Drug Deliv Rev. 2022;188:114396. https://doi.org/10.1016/j.addr.2022.114396.

62. Mandl HK, Quijano E, Suh HW, Sparago E, Oeck S, Grun M, Glazer PM, Saltzman WM. Optimizing biodegradable nanoparticle size for tissue-specific delivery. J Control Release. 2019;314:92-101. https://doi.org/10.1016/j.jconrel.2019.09.020.

63. Alakhova DY, Kabanov AV. Pluronics and MDR reversal: An update. Mol Pharmaceut. 2014;11(8):2566-2578. https://doi.org/10.1021/mp500298q.

64. Erstad DJ, Sojoodi M, Taylor MS, Ghoshal S, Razavi AA, Graham-O'Regan KA, Bardeesy N, Ferrone CR, Lanuti M, Caravan P, Tanabe KK, Fuchs BC. Orthotopic and heterotopic murine models of pancreatic cancer and their different responses to FOLFIRINOX chemotherapy. Dis Model Mech. 2018;11(7). https://doi.org/10.1242/dmm.034793.

65. Guo DD, Hong SH, Jiang HL, Kim JH, Minai-Tehrani A, Kim JE, Shin JY, Jiang T, Kim YK, Choi YJ, Cho CS, Cho MH. Synergistic effects of Akt1 shRNA and paclitaxel-incorporated conjugated linoleic acid-coupled poloxamer thermosensitive hydrogel on breast cancer. Biomaterials. 2012;33(7):2272-2281. https://doi.org/10.1016/j.biomaterials.2011.12.011.

66. Zhao D, Song H, Zhou X, Chen Y, Liu Q, Gao X, Zhu X, Chen D. Novel facile thermosensitive hydrogel as sustained and controllable gene release vehicle for breast cancer treatment. Eur J Pharm Sci. 2019;134:145-152. https://doi.org/10.1016/j.ejps.2019.03.021.